

Temperature-Dependent Surface States and Transitions of Si(111)-7×7

J. E. Demuth, B. N. J. Persson, and A. J. Schell-Sorokin

IBM Thomas J. Watson Research Center, Yorktown Heights, New York 10598

(Received 28 September 1983)

uv photoemission and electron-energy-loss measurements of Si(111)-7×7 between $T = 15$ and 300 K reveal significant temperature-dependent changes in the occupied surface states and their transitions which can be associated with electron-phonon coupling at the surface. Several new surface states and transitions are determined at low temperatures, including a highly localized (~ 2 -meV-wide), half-occupied state that resides within a 100-meV-wide surface-state band gap and determines the Fermi-level position.

PACS numbers: 73.20.Cw, 79.20.Hx, 79.60.Eq

Considerable interest exists in understanding the nature and origin of semiconductor surface reconstruction as well as the details of Fermi-level pinning at semiconductor surfaces and interfaces. Numerous room-temperature spectroscopic studies of these surfaces have been performed and, almost exclusively compared to "rigid lattice" (i.e., $T=0$) electronic structure calculations for insight into the electronic states, bonding, and geometric structure. Here, we present the first low-temperature spectroscopic studies of any silicon surface—Si(111)-7×7—which demonstrate that finite-temperature effects exist on semiconductor surfaces which may limit our physical understanding of them. Specifically, we show that at low temperatures the Si(111)-7×7 surface has several surface states near the Fermi level and low-lying surface-state transitions which have not been previously observed.¹⁻⁶ Our temperature-dependent measurements suggest that the "metalliclike" characteristics of Si(111)-7×7 observed at room temperature¹⁻⁵ arise from electron-phonon coupling, together with a highly localized, half-occupied state at the Fermi level. Thus, these results not only provide a different physical picture of Si(111)-7×7 and new data for comparison to electronic structure calculations, but are the first experimental results to support the prediction of significant electron-phonon coupling and its importance at semiconductor surfaces.⁷

These measurements were performed in an ion-/turbomolecular-/titanium sublimator-pumped ultrahigh-vacuum system having a base pressure of 4×10^{-11} Torr. This system contains a cylindrical mirror analyzer (CMA) for Auger and ultraviolet photoemission spectroscopy (UPS), a three-grid Varian low-energy electron-diffraction (LEED) optics, and a set of hemispherical deflection analyzers (2.5-cm diam.) for high-resolution electron-energy-loss measurements (EELS). A boron-doped sample (1.3×10^{15} atoms/

cm²) was ultrasonically machined, mechanically and chemically polished, and physically clamped to the sample support by a Ta retaining ring.

The sample could be indirectly cooled and heated between 15 and 1400 K as measured with a Chromel-Alumel thermocouple spot welded to the retaining ring. Cooling of the sample was preceded by cooling of the cryostat which reduced system pressures below 2×10^{-11} Torr and virtually eliminated ambient contamination during cool-down and measurements. The sample was cleaned by initial argon-ion bombardment (400 V) followed by *repeated* oxidation cycles, annealing to 1350 K, and slow cooling to produce atomically clean, well-ordered, low-background 7×7 surfaces.

UPS was done at 21.2 and 40.8 eV in an angle-integrating mode with the light source 90° from the axis of the CMA and a <211> direction of the sample normal to the plane of incidence. The sample normal could be rotated about this <211> direction and was positioned between 35° and 60° from the CMA axis. A 2000-Å Al foil was used to filter out the visible light produced in the resonance lamp and confirmed that no visible-photon-induced effects altered the UPS spectra. The sample Fermi-level position (E_F) was determined by looking at the Ta retaining ring. The UPS resolution function was determined to be ~ 180 meV full width at half maximum (FWHM) from the broadening of the Fermi level of Ta.

EELS was done with a fixed total scattering angle of 90° with specular scattering conditions ($\theta_i = \theta_o = 45^\circ$) and incident beam energies (12–20 eV) where optical (dipole) selection rules are applicable. Off-specular measurements confirm that the features we report here are dipole excited. Our EELS resolution, as determined after reflection from the crystal, was typically 7–9 meV (FWHM) but was degraded to 20 meV to examine the lower-intensity losses above $\frac{1}{2}$ eV.

In Fig. 1, we show the He I-excited ($h\nu = 21.2$

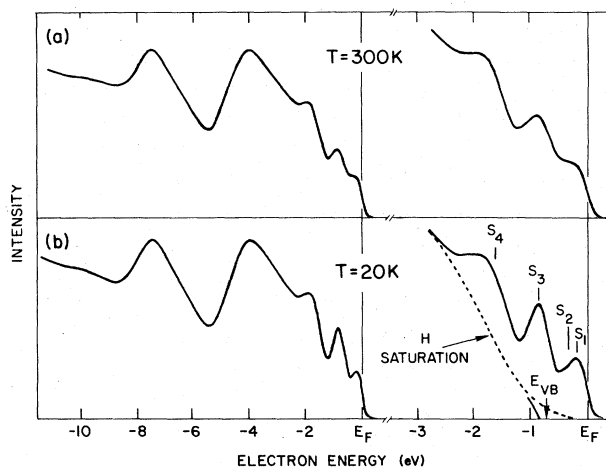


FIG. 1. Ultraviolet photoemission spectra ($h\nu=21.2$ eV) for Si(111)- 7×7 at (a) 300 K and (b) 20 K under identical conditions. The right panels show an expanded view of the surface states near the top of the valence band.

eV) photoemission spectra of Si(111)- 7×7 (a) at room temperature (RT) and (b) after cooling to 20 K. Although the valence bands below 3 eV are unchanged upon cooling, we observe marked intensity changes and a continuous sharpening of the surface states near E_F as the temperature is reduced. The temperature dependence we observe in these surface states also occurs for $h\nu=40.8$ eV, is reversible with temperature cycling, and is not sensitive to small concentrations of atomic hydrogen. The changes in the high-lying surface states at RT correspond to a 0.25-eV broadening of the low-temperature features as deduced from the 0.1-eV broadening of the S_3 state between 20 and 300 K. At $T\sim 20$ K the highest-lying surface state forms a peak, S_1 , ~ 150 meV below E_F , with a possible shoulder S_2 at ~ 250 meV. These low-temperature results immediately raise questions as to whether this surface is metallic as previously proposed¹⁻⁵ as well as the nature and number of surface states near E_F . Our temperature-dependent EELS results resolve these questions and provide more insight into the possible origin of these temperature-dependent changes.

Temperature-dependent loss spectra are shown in Fig. 2. Both the broadening of the elastic peak and the continuumlike background are strongly reduced at low temperatures to reveal five well-defined peaks at 63, 95, ~ 210 , ~ 340 , and ~ 900 meV (labeled as T_0 to T_4 , respectively). Numerous experiments reveal that these features are

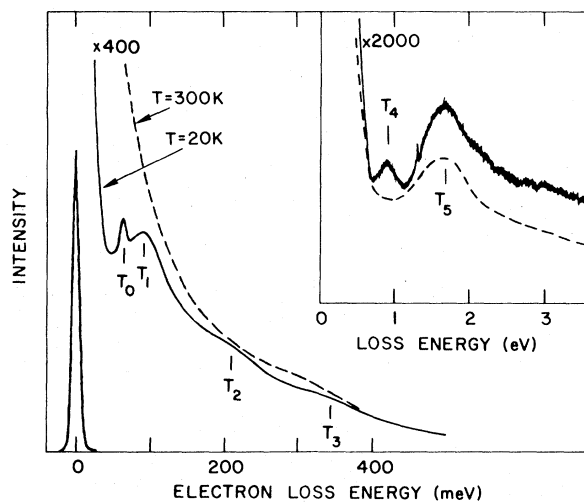


FIG. 2. Electron-energy-loss spectra for $E_B=15$ eV at $T=300$ K (dashed lines) and $T=20$ K (solid lines). In the inset the resolution has been degraded to 20 meV (FWHM).

intrinsic and not derived from condensed or trace contaminants (e.g., H_2 , C, CO, CH_4 , CO_2 , etc.). For example, the sharp 63-meV feature is markedly attenuated by small levels of contamination and/or structural imperfection, and by analogy to Si(111)- 2×1 , can be attributed to a surface phonon.⁸ This value is slightly larger than the 57 meV observed on Si(111)- 2×1 and may reflect the additional rigidity of a two-dimensional bonding array proposed in the π -bonding chain model for 2×1 -Si(111).⁹ The broader features T_1 to T_4 also disappear with higher adsorbate coverage and can be attributed to interband transitions between surface states of Si(111)- 7×7 . The T_5 transition at 1.7 eV has some surface-state character but is not completely attenuated upon adsorption because of the occurrence of bulk (direct gap) transitions in this same energy region.¹⁰ We note that recent optical studies¹¹ also support an assignment of T_3 to a direct interband transition rather than to a surface plasmon.⁵

For greater insight into these temperature-dependent changes, we reduce our EELS data to account for the finite collection angle, resolution, and scattering kinematics, and present the surface loss function, $\text{Im}\bar{g}$,¹² shown in Fig. 3. Here we consider and subtract out the elastic tail and weaker bulk excitations as determined from identical measurements of a H-covered surface at $T=15$ K. These results suggest the existence of an ~ 40 -meV energy gap between occupied and unoccupied surface states at low temperatures.

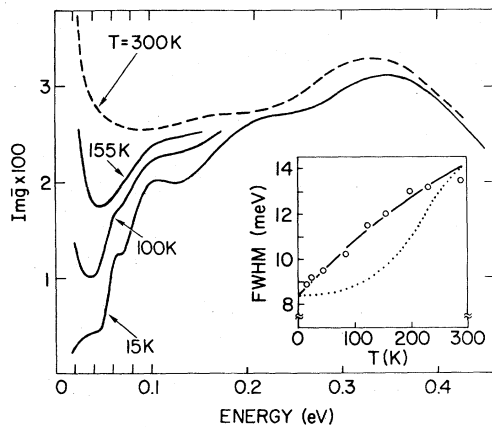


FIG. 3. The surface loss function, $\text{Im}\bar{g}(E)$, at several temperatures as derived from data with $E_B = 12$ eV, $\theta_i = \theta_0 = 45^\circ$, a measured angular acceptance of 2° , and a total instrumental resolution of 8.5 meV (FWHM). For $T = 15$ K, the integral of $\text{Im}\bar{g}$ up to ~ 0.5 eV has an oscillator strength corresponding to 4–5 electrons per 7×7 unit cell (Ref. 13) while the “foot” below 40 meV may reflect band tailing or other phonons which we have neglected in our analysis. The inset shows the temperature-dependent variation of the elastic beam (circles) and two possible processes for beam broadening. The solid line corresponds to a constant free-carrier concentration while the dotted line corresponds to thermally activated free carriers associated with a 40-meV surface-state gap.

The presence of such a gap would be expected to produce thermally activated surface free carriers and low-energy plasmon excitations, which could produce the temperature-dependent broadening of the elastic beam. To evaluate this possibility further we have analyzed the temperature-dependent width of the quasielastic peak using a multiple-scattering analysis as described elsewhere.¹³ In this analysis the surface free-carrier density n and effective mass m^* enter as a ratio n/m^* . For the case of thermally excited carriers, we anticipate strongly reduced beam broadening at low temperatures when surface carrier “freezeout” occurs. Assuming a surface state gap of 40 meV and fitting the theoretically derived beam broadening to our room-temperature measurement, we predict the temperature-dependent broadening shown by the dotted line in the inset of Fig. 3. In contrast we find that the experimental broadening is well described by a constant carrier density, as shown by the solid line. For this case the reduced broadening at low temperatures arises from the temperature dependence of the Bose-Einstein factors in the inelastic-scattering cross section.¹⁴ Given the

ratio of n/m^* , the assumption of $\sim 2m_0$ gives a density of 8×10^{-4} electrons per surface atom which would correspond to one electron per ~ 25 unit cells of the 7×7 surface. Since this background and elastic beam broadening is reproducible and has been achieved by other groups using different methods of preparation,⁵ we believe that it is intrinsic to the 7×7 structure. Consideration of the existence of a unique site per 7×7 surface unit cell¹⁵ and our observation of the disappearance of the elastic beam broadening at comparable hydrogen coverages ($\sim 5\%$ of a monolayer) lead us to propose that this electron density likely arises from one electron per 7×7 unit cell and $m^* \sim 50m_0$. This large effective mass implies a very localized, narrow (~ 2 meV) state at E_F which must be half-occupied to provide free carriers. Such a sharp feature would be influenced by many-body effects which, for example, can produce a magnetic ground state as discussed elsewhere.¹³ The 40-meV gap we determine from $\text{Im}\bar{g}$, as well as the T_1 transition, then arises from transitions to or from this localized state to the more delocalized surface-state band edges. The energy gap of these more delocalized surface states is ~ 100 meV, as determined upon removal of this localized state and the T_1 transition by small amounts of atomic hydrogen. The T_2 , T_3 , T_4 , and T_5 transitions remain and appear to be surface-state transitions from the S_1 to S_4 surface states, respectively, to an unoccupied state ~ 50 meV above E_F . Such an assignment is supported by the correlated extinction of certain surface states and transitions with different adsorbates (e.g., S_3 and T_4 with H_2O), and is in agreement with surface photovoltage results.⁶

The temperature-dependent changes we observe in both UPS and EELS are not accompanied by any significant temperature-dependent changes in LEED patterns, relative spot intensities, or intensity energy profiles (e.g., LEED analysis of the 00 beam suggests no changes in d_\perp within ± 0.003 Å). These continuous changes also provide little evidence for an insulator-metal phase transition over these temperatures, which has been discussed as a mechanism for reconstruction.^{16,17} We attribute both the temperature-dependent broadening of our UPS and EELS features as well as the temperature-dependent shift of several surface-state transitions to the existence of electron-phonon coupling at the surface as is known to occur in the bulk.^{7,18} Our results suggest slightly stronger e - p coupling at the clean surface than in the bulk, i.e., e - p lifetime broad-

ening as large as ~ 250 meV and shifts in the surface-state transition of 40–70 meV, as compared to the 45-meV bulk–band-gap change between 0 and 300 K.¹⁹

In summary, we demonstrate the complexities of finite-temperature effects on measured semiconductor surface electronic structure and the general need for low-temperature measurements. In particular we show that the Si(111)- 7×7 surface has an unusual surface electronic structure where a highly localized, half-occupied state exists in a surface-state band gap and determines the position of E_F . Evidence suggests that this localized state is intrinsic to the 7×7 structure and may be associated with the odd number of electrons and/or a single missing atom per 7×7 unit cell.²⁰

The authors wish to acknowledge useful discussions with K. C. Pandey, F. J. Himpsel, and F. Stern, and to thank the U. S. Office of Naval Research for partial support of this work.

¹G. Chiarotti, P. Chiaradia, and S. Nannarone, *Surf. Sci.* **49**, 315 (1975).

²D. E. Eastman, F. J. Himpsel, and J. F. van der Veen, *Solid State Commun.* **35**, 345 (1980).

³D. J. Chadi, R. S. Bauer, R. H. Williams, G. V.

Hansson, R. Z. Bachrach, J. C. Mikkelsen, Jr., F. Houzay, G. M. Guichov, R. Pinchaux, and Y. Petroff, *Phys. Rev. Lett.* **44**, 799 (1980).

⁴F. J. Himpsel, D. E. Eastman, P. Heimann, B. Reihl, C. W. White, and D. M. Zehner, *Phys. Rev. B* **24**, 1120 (1981).

⁵U. Backes and H. Ibach, *Solid State Commun.* **40**, 575 (1981).

⁶J. Clabes and M. Henzler, *Phys. Rev. B* **21**, 625 (1980).

⁷Francisco Guinea and Carlos Menéndez, *Phys. Rev. B* **27**, 1432 (1983).

⁸H. Ibach, K. Horn, R. Dorn, and H. Lüth, *Surf. Sci.* **38**, 433 (1973).

⁹K. C. Pandey, *Phys. Rev. Lett.* **47**, 1913 (1981).

¹⁰J. E. Rowe and H. Ibach, *Phys. Rev. Lett.* **31**, 102 (1973).

¹¹Y. J. Chabal, *Bull. Am. Phys. Soc.* **28**, 860 (1983).

¹²B. N. J. Persson, *Phys. Rev. Lett.* **50**, 1089 (1983).

¹³B. N. J. Persson and J. E. Demuth, to be published.

¹⁴A. A. Lucas and M. Sunjic, *Prog. Surf. Sci.* **2**, 75 (1977); W. L. Schaich, *Surf. Sci.* **122**, 175 (1982).

¹⁵Y. J. Chabal, *Phys. Rev. Lett.* **50**, 1850 (1983).

¹⁶E. Tosatti and P. W. Anderson, *Solid State Commun.* **14**, 773 (1974).

¹⁷A. Muramatsu and W. Hanke, *Solid State Commun.* **42**, 537 (1982).

¹⁸P. B. Allen and M. Cardona, *Phys. Rev. B* **27**, 476 (1983).

¹⁹W. Bludau, A. Onton, and W. Heinke, *J. Appl. Phys.* **45**, 1846 (1974).

²⁰G. Binnig and H. Rohrer, *Phys. Rev. Lett.* **50**, 120 (1983).